J|A|C|S COMMUNICATIONS

Published on Web 10/20/2009

# Tin Nanoparticles Encapsulated in Porous Multichannel Carbon Microtubes: Preparation by Single-Nozzle Electrospinning and Application as Anode Material for High-Performance Li-Based Batteries

Yan Yu,*,† Lin Gu,*,‡ Changbao Zhu,† Peter A. van Aken,‡ and Joachim Maier†

*Max Planck Institute for Solid State Research, Heisenbergstr. 1, 70569 Stuttgart, Germany, and Stuttgart Center for Electron Microscopy, Max Planck Institute for Metals Research, Heisenbergstr. 3, 70569 Stuttgart, Germany*

Received July 31, 2009; E-mail: yan.yu@fkf.mpg.de; gu@mf.mpg.de

Rechargeable lithium ion batteries are one of the favorite energy storage devices for upcoming mobile electric devices and hybrid vehicles because of their high energy density and long cycle lifetime.[1] Tin metal has been proposed as one of the most promising anode candidates because of its high theoretical capacity of ~992 mAh $g^{-1}$ (formation of $Li_{4.4}Sn$).[2,3] However, implementation of metallic tin for lithium ion battery applications has been greatly hampered by the poor cyclability resulting from both pulverization of particles and electrical disconnection from the current collector caused by the large volume variation during the lithium alloying and dealloying processes.[4] Substantial efforts have been made to increase its performance, including modifying the electrode configuration, decreasing the particle size,[5] using thin films,[6] and selecting optimized binders.[7] Recently, considerable attention has been focused on reducing such volume change by forming composite materials of carbon and Sn nanoparticles[8,9] as well as designing tin-encapsulated hollow spherical carbon structures.[10−13] It was demonstrated that the poor cyclability of the tin electrodes can be improved by using nanoscaled tin−carbon composite materials and a nanoscale current-collector design.[14] These approaches are not optimal because of a considerably low proportion of functional active species.

In this work, we greatly improved the electrochemical performance of Sn−C electrodes by forming metallic Sn particles encapsulated in porous multichannel carbon microtubes (denoted as SPMCTs) using a single-nozzle electrospinning technique and subsequent calcination. In this way, an appropriate compromise between a high packing density of tin particles and sufficient space to buffer the volume variation can be realized. Furthermore, the porous carbon shell maintains the stability of the structural arrangements, avoids oxidation of Sn, serves as an electron supplier, and allows $Li^+$ access.[15−17] In addition, we demonstrate that single-nozzle electrospinning is a powerful alternative among electrospinning techniques[18] that does not involve a complex formulation of the necessary solutions[18] to produce a one-dimensional core−sheath structure.

Figure 1a gives a sketch of the electrospinning process of tin octoate−poly(methyl methacrylate) (PMMA)−polyacrylonitrile (PAN) in DMF emulsion. It has been demonstrated that a PAN solution is easier to stretch than a PMMA/DMF fluid, which can be pulled into the PAN/DMF jet, thus leading to the formation of a core−shell jet and the subsequent formation of core−shell fibers.[19] As a result, the shell of the as-spun fiber consists of PAN while the core region consists of tin octoate−PMMA composite. The scanning electron microscopy (SEM) image in Figure 1b reveals the morphology of the as-electrospun fibers, which display a uniform diameter distribution of ~3 $\mu$m. As shown in Figure 1c, the as-collected electrospun fibers were first stabilized in air at 250 °C, leading to a thermal degradation of the core components (tin octoate−PMMA) to create $SnO_2$ nanoparticles encapsulated in porous hollow fibers. After carbonization under an $Ar/H_2$ atmosphere, the fibers were transformed into multichannel hollow porous carbon microtubes with an average diameter of ~2 $\mu$m (Figure S1 in the Supporting Information). Figure 1d displays the cross section of the same fibers after carbonization, showing the multichannel tubular structure with an average channel diameter of ~150 nm. The average thickness of the channel walls is ~100 nm with many small holes (diameter ~100 nm) embedded.

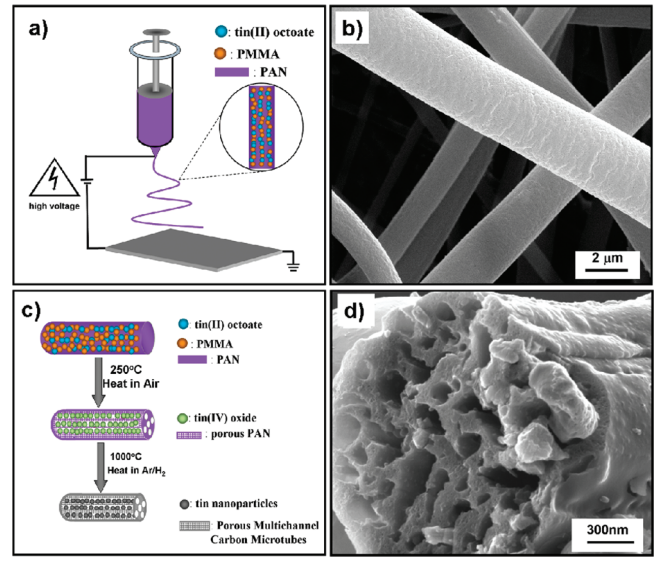


***Figure 1.*** (a) Schematic illustration of coelectrospinning of a PMMA−PAN−tin octoate mixture in DMF using a single-needle nozzle. The inset (right) shows magnified details of the needle orifice shown in black. In the inset, the PMMA/DMF droplets are shown in orange, while the PAN/DMF liquid and tin octoate are shown in purple and dark-blue, respectively. (b) SEM micrographs of the as-collected core−shell nanofibers obtained via the single-nozzle electrospinning technique. (c) Proposed synthetic scheme for Sn nanoparticles encapsulated in porous multichannel carbon microtubes (SPMCTs). (d) High-magnification cross-sectional image of carbonized PMMA−PAN−tin octoate nanofibers that reveals the tubular structure of the SPMCTs.

Figure 2a shows Sn nanoparticles with a diameter of ~200 nm encapsulated in nearly all of the channels of the hollow carbon microfibers (diameter ~2 $\mu$m). A magnified image (Figure 2b) reveals the channel walls (i.e., the carbon fibers) to be porous with a relatively uniform size distribution of ~100 nm in diameter. A high-resolution transmission electron microscopy (HRTEM) micrograph, shown in Figure 2c, displays the fine microstructure of

† Max Planck Institute for Solid State Research.
‡ Max Planck Institute for Metals Research.



10.1021/ja906261c CCC: $40.75 

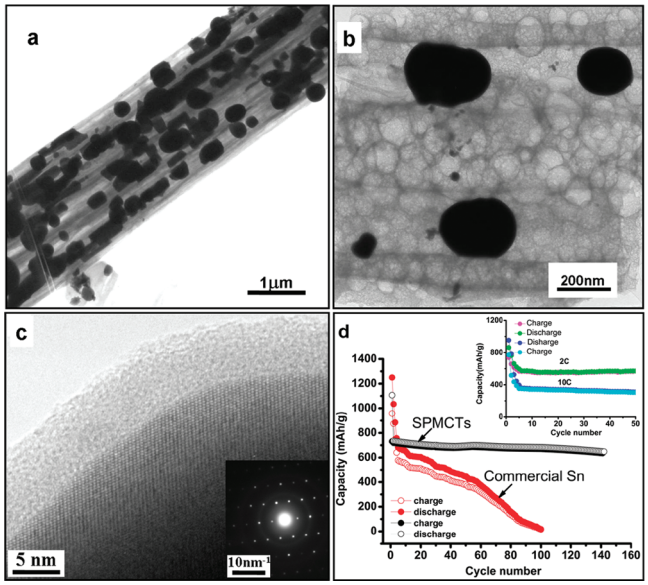


***Figure 2.*** (a) TEM micrograph of the converted Sn encapsulated in multichannel carbon microtubes after heat treatment under an $Ar/H_2$ atmosphere. (b) HRTEM image confirming the porous multichannel walls. (c) HRTEM micrograph and SAED pattern of an isolated Sn nanoparticle, revealing the presence of single-crystalline metallic tin and amorphous carbon. (d) Cyclibility of SPMCTs and commercial Sn nanopowder with similar sizes (~200 nm) at a cycling rate of 0.5 C (current density 100 mA $g^{-1}$); the inset displays the discharge capacities of SPMCT electrodes as a function of discharge rate at 2 and 10 C. All of the batteries were cycled in a voltage window of 5 mV to 2 V.

metallic tin nanoparticles coated by a thin carbon layer with a thickness of ~5 nm. The spot- and ringlike patterns in the selected-area electron diffraction (SAED) pattern (inset of Figure 2c) confirm the presence of single-crystalline tin and amorphous carbon. X-ray diffraction (XRD) patterns of the SPMCTs (Figure S2) indicate complete reduction to form metallic tin (JCPDS file no. 01-086-2264). Energy-dispersive X-ray spectroscopy (EDX) analyses after absorption corrections (Figure S3 and Table S1) revealed that the SPMCTs contain 32 wt % carbon and 66 wt % tin. Figure 2d compares the cycle performance of electrochemical cells made of the SPMCTs and commercial Sn nanoparticles with diameters of ~200 nm at a constant current density of 100 mA $g^{-1}$ (~0.5 C) in the voltage range 0.005−2.0 V (vs Li). A 30% capacity loss of the first cycle was observed, after which the charge−discharge efficiency approached ~100% (Figure 2d). Notably, the maximum capacity of the SPMCTs was calculated to be 774.4 mAh $g^{-1}$. The SPMCT electrode provided a reversible discharge capacity as high as 648 mAh $g^{-1}$ (83.7% of the theoretical capacity) even after 140 cycles, whereas the commercial Sn nanoparticle electrode could be cycled only ~20 times before rapid degradation occurred. Furthermore, as shown in the inset of Figure 2d, the SPMCT electrode showed an excellent rate capability at discharge rates of 2 and 10 C, with an even more stable cycling performance. The specific capacity was found to be 570 mAh $g^{-1}$ at 2 C and 295 mAh $g^{-1}$ at 10 C after 50 cycles, which correspond to 73.6 and 38.1% retention of the theoretical capacity, respectively. The performance was also substantially better than that of Sn−C composites reported in the literature to date.[12,17] To show the improved electrochemical performance of our Sn−C composite, we also tested a full cell in which the Sn−C electrode was coupled with a commercial $LiCoO_2$ cathode in a 1 M $LiPF_6$ (EC/DEC) electrolyte solution. The cyclability was excellent (Figure S4).

In summary, we have reported a novel Sn−C composite with a core−shell morphology of Sn nanoparticles encapsulated in porous multichannel carbon microtubes that was fabricated by a single-nozzle electrospinning technique. This material exhibited excellent characteristics in terms of reversible capacities, cycling performance, and rate capability for applications as an anode material in Li-based batteries. Moreover, encapsulation of nanoparticles in porous multichannel carbon tubes by single-nozzle electrospinning provides a useful platform for designing and constructing high-performance electrode materials for Li-based batteries or supercapacitors. As the fibers are porous throughout, they are also well-suited to encapsulate substances that are of interest for catalysis.

**Acknowledgment.** Y.Y. is grateful for the scholarship from the Alexander von Humboldt Foundation.

**Supporting Information Available:** Detailed experimental methods and SEM, XRD, and EDX analyses. This material is available free of charge via the Internet at http://pubs.acs.org.

## References

(1) Tarascon, J. M.; Armand, M. *Nature* **2001**, *414*, 359–367.
(2) (a) Winter, M.; Besenhard, J. O. *Electrochim. Acta* **1999**, *45*, 31–50. (b) Yang, J.; Winter, M.; Besenhard, J. O. *Solid State Ionics* **1996**, *90*, 281–287.
(3) (a) Courtney, I. A.; Dahn, J. R. *J. Electrochem. Soc.* **1997**, *144*, 2045–2052. (b) Whitehead, A. H.; Elliott, J. M.; Owen, J. R. *J. Power Sources* **1999**, *81−82*, 33–38.
(4) Li, H.; Shi, L.; Wang, Q.; Chen, L.; Huang, X. *Solid State Ionics* **2002**, *148*, 247–258.
(5) Besenhard, J. O.; Yang, J.; Winter, M. *J. Power Sources* **1997**, *68*, 87–90.
(6) Wilson, A. M.; Dahn, J. R. *J. Electrochem. Soc.* **1995**, *142*, 326–332.
(7) Wachtler, M.; Wagner, M. R.; Schmied, M.; Winter, M.; Besenhard, J. O. *J. Electroanal. Chem.* **2001**, *510*, 12–19.
(8) (a) Zhang, W. M.; Hu, J. S.; Guo, Y. G.; Zheng, S. F.; Zhong, L. S.; Song, W. G.; Wan, L. J. *Adv. Mater.* **2008**, *20*, 1160–1165. (b) Hassoun, J.; Derrien, G.; Panero, S.; Scrosati, B. *Adv. Mater.* **2008**, *20*, 3169–3175.
(9) (a) Cui, G. L.; Hu, Y. S.; Zhi, L. J.; Wu, D. Q.; Frieberwirth, I.; Maier, J.; Müllen, K. *Small* **2007**, *3*, 2066–2069. (b) Egashira, M.; Takatsuji, H.; Okada, S.; Yamaki, J. *J. Power Sources* **2002**, *107*, 56–60.
(10) Lee, K. T.; Jung, Y. S.; Oh, S. M. *J. Am. Chem. Soc.* **2003**, *125*, 5652–5653.
(11) Jung, Y. S.; Lee, K. T.; Ryu, J. H.; Im, D.; Oh, S. M. *J. Electrochem. Soc.* **2005**, *152*, A1452–A1457.
(12) Derrien, G.; Hassoun, J.; Panero, S.; Scrosati, B. *Adv. Mater.* **2007**, *19*, 2336–2340.
(13) Guo, B. K.; Shu, J.; Tang, K.; Bai, Y.; Wang, Z. X.; Chen, L. Q. *J. Power Sources* **2008**, *177*, 205–210.
(14) (a) Hassoun, J.; Panero, S.; Simon, P.; Taberna, P. L.; Scrosati, B. *Adv. Mater.* **2007**, *19*, 1632–1635. (b) Bazin, L.; Mitra, S.; Taberna, P. L.; Poizot, P.; Gressier, M.; Menu, M. J.; Barnabé, A.; Simon, P.; Tarascon, J. M. *J. Power Sources* **2009**, *188*, 578–582.
(15) Hassoun, J.; Derrien, G.; Panero, S.; Scrosati, B. *Electrochim. Acta* **2009**, *54*, 4441–4444.
(16) Huang, H.; Yang, S.; Gu, G. *J. Phys. Chem. B* **1998**, *102*, 3420–3424.
(17) (a) Deng, D.; Lee, J. Y. *Chem. Mater.* **2008**, *20*, 1841–1846. (b) Deng, D.; Lee, J. Y. *Angew. Chem., Int. Ed.* **2009**, *48*, 1660–1663.
(18) (a) Loscertales, I. G.; Barrero, A.; Guerrero, I.; Cortijo, R.; Marquez, M.; Gañán-Calvo, A. M. *Science* **2002**, *295*, 1695–1698. (b) Li, D.; Xiao, Y. *Nano Lett.* **2004**, *4*, 933–938. (c) Zussman, E.; Yarin, A. L.; Bazilevsky, A. V.; Avrahami, R.; Feldman, M. *Adv. Mater.* **2006**, *18*, 348–353.
(19) Bazilevsky, A. V.; Yarin, A. L.; Megaridis, C. M. *Langmuir* **2007**, *23*, 2311–2314.

JA906261C